minerals

MDPI

Article

Agates from Kerrouchen (The Atlas Mountains, Morocco): Textural Types and Their Gemmological Characteristics

Lucyna Natkaniec-Nowak [1], Magdalena Dumańska-Słowik [1,*], Jaroslav Pršek [1], Marek Lankosz [2], Paweł Wróbel [2], Adam Gaweł [1], Joanna Kowalczyk [1] and Jacek Kocemba [1]

[1] Faculty of Geology, Geophysics and Environmental Protection, Department of Mineralogy, Petrography and Geochemistry, AGH University of Science and Technology, 30 Mickiewicza av., 30-059 Kraków, Poland; natkan@agh.edu.pl (L.N.-N.); prsek@yahoo.com (J.P.); agawel@agh.edu.pl (A.G.); joanna.j.kowalczyk@gmail.com (J.K.); jacooo88@gmail.com (J.K.)

[2] Faculty of Physics and Applied Computer Science, AGH University of Science and Technology, 30 Mickiewicza av., 30-059 Kraków, Poland; mlankosz@agh.edu.pl (M.L.); pawel.wrobel@fis.agh.edu.pl (P.W.)

* Correspondence: dumanska@agh.edu.pl

Academic Editor: Raymond M. Coveney, Jr.
Received: 30 April 2016; Accepted: 7 July 2016; Published: 26 July 2016

Abstract: Agate nodules from Kerrouchen (Khénifra Province, Meknés-Tafilalet Region) in Morocco occur in Triassic basalts and reach up to 30 cm in diameter. Monocentric, banded agates—mainly in pastel pink, grey, white and yellow—with infiltration canals (*osculum*) are observed. Raman microspectroscopy revealed that the agates mainly consist of low quartz and subordinately moganite with distinctive 460 and 501 cm^{-1} marker bands, respectively. Linear mapping indicated that moganite mainly concentrates in grey zones of the monocentric agate nodules. The other types, polycentric and pseudostalactitic agates, are usually brown and red and contain minerals such as hematite and goethite. They form both regular and irregular mosaics rich in ornamentation. Occasionally, aggregates of copper sulphides or titanium oxides (rutile) can also be observed. These minerals are sometimes accompanied by carbonaceous material marked by 1320 and 1585 cm^{-1} Raman bands. It seems that formation of agates from Kerrouchen was induced by Si-rich and Fe-moderate fluids. Copper sulphides, rutile, and carbonates (possibly calcite) were most likely incorporated during post-magmatic processes. The origin of solid bitumen can be the result of hydrothermal or hypergenic processes.

Keywords: agate; Kerrouchen; Morocco; colour pigments; microtexture

1. Introduction

The crystallization of agates worldwide has proceeded for millions of years. The oldest gems were found in Pilbara rock formations (3500–2700 Ma) and the youngest originated from volcanic tuffs from the Yucca Mt. in the USA (13 Ma) [1]. The genesis of agates is strictly connected with volcanic and hypergenic solutions, which are the source of various ions and organic matter. The most common origin of agates is a complex, multi-stage silica crystallization from these solutions with changing chemical composition [2] or cyclic crystallization of pigments from the silica gel in the pores of volcanic rocks [3]. Generally, formation of agates takes place in volcanic rocks, hydrothermal veins, or in sediments. In basic volcanic rocks they crystallize in vesicles of former gas or fluid bubbles. In contrast, agate genesis in acidic volcanic host rocks starts with the formation of lithophysae (high-temperature crystallization domains). Agates form in holes of these lithophysae, which are the result of tensional stress and/or degassing and crystallization in the cooling melt [4]. As a result, agate

occurs in different forms—usually they are the same as the original pores in the host rocks, but may undergo pseudomorphosis after different primary minerals such as calcite or barite. The central part of the geode is very often filled with different cryptocrystalline quartz varieties—amethyst, smoky quartz, prasiolite, rock crystals, or morion. Agate nodules can reach diameters from several centimetres up to several tenths of centimetres, and can reach weights of up to several hundreds of kilograms.

During the last decades, agates from Morocco have become interesting gems among mineral collectors. Agates occur in the Triassic basalts at many localities in the High Atlas–Sidi Rahal [3–5], Asni, Tizi-n-Tichka area, Agouim, Ahouli, and Kerrouchen [6–9]. The agates from each locality have unique characteristics, such as type and colour, as well as the general pattern revealed on its polished section. All of them can reach up to 30 cm in diameter. Sidi Rahal and Asni agates have greyish-white, bluish-white, or red to brown colours, whereas agates from Kerrouchen show a diversity of colours in the individual zones from the white to grey, yellow, orange, blue, red, and even brown in one sample. The agate geodes from Kerrouchen are also unique by their variety of patterns and morphological structures. They are mainly monocentric, subordinately polycentric to pseudostalactitic. Monocentric banded agates or horizontally stratified agates are rarities. Agates with stalactites similar to the so-called "plume" agates from Texas (USA) are the most sought-after in that country. The other popular forms of agates are white agates—Cacholong ("kalmuck agate") with blue-grey or pinkish chalcedony zones—or agates with "Wagler effect" (i.e., three-dimensional chatoyant effect), which can be also found in the Kerrouchen area [6].

The first geological descriptions of agates from the Atlas Mountains were made in the 1940s (vide [6–8]). However, the "agate fever" did not start there until of the 20th century.

However, such interest in Moroccan agates by collectors worldwide has not resulted in the increased amounts of the scientific publications. Recent articles mainly contain descriptions of agates' localities in the High Atlas Mountains, with focus placed on general geology of the region or on the exploration of these ornamental stones for jewellery (e.g., [5,6,8–13]). A more complex mineralogical study of agates from Sidi Rahal was conducted by Dumańska-Słowik et al. [3]. This study described, in detail, the internal texture of the agates as well as number and character of solid inclusions found in them.

In the present study, continuing the research on Moroccan agates, the distribution of different silica phases in rhythmically zoned agates from Kerrouchen, together with the characteristic of solid inclusions occurring in their coloured zones, are presented. To ascertain the agates' formation, we have applied optical transmission microscopy, scanning electron-microscopic observations (SEM-EDS) supported by Raman microspectroscopy (RS), and X-ray fluorescence analysis (XRF).

2. Geological Setting

Morocco is situated in a western part of the folded Atlas Mountains, which cover an area of more than 2000 km long from the Atlantic coastline to Kabiska Bay in the Mediterranean area. These mountains are the elongations of the European Alpine orogenic system. The Atlas Unit was formed, folded, and dislocated at the beginning of Paleogene. It consists of two main folded units: the internal with Middle, High Atlas, Sahara Atlas, and Anti-Atlas [14], and the external with Tell Atlas and Rif [15]. These units are divided by Morocco Meset (200–1500 m a.s.l.) and Shott Plane (750–1000 m a.s.l.).

The High Atlas is built by Paleozoic rocks—crystalline schists, quartzites, limestones, and Hercynian volcanic rocks. The upper parts are covered by huge layers of folded Jurassic and Cretaceous limestones with Lower Paleogen limestones and sandstones. The areas richest in agates are: Tizi-n-Tichka, Asni and Sidi Rahal [6]. The agate deposit in Kerrouchen was found at the beginning of this century. This small village is situated in the Khénifra Province (Middle Morocco) and is surrounded by the High Atlas to the south, Rif Mountains to the north, and Wadi Muluja valley to the east (Figure 1). The agates can be collected on the mountain slopes, in the agricultural fields, as well as along the road running from Bouma to Kerrouchen. They are found within the Triassic and Lower Jurassic volcanic rocks–basalts, whose outcrop in the area in the form of a crescent 10 × 20 km in size.

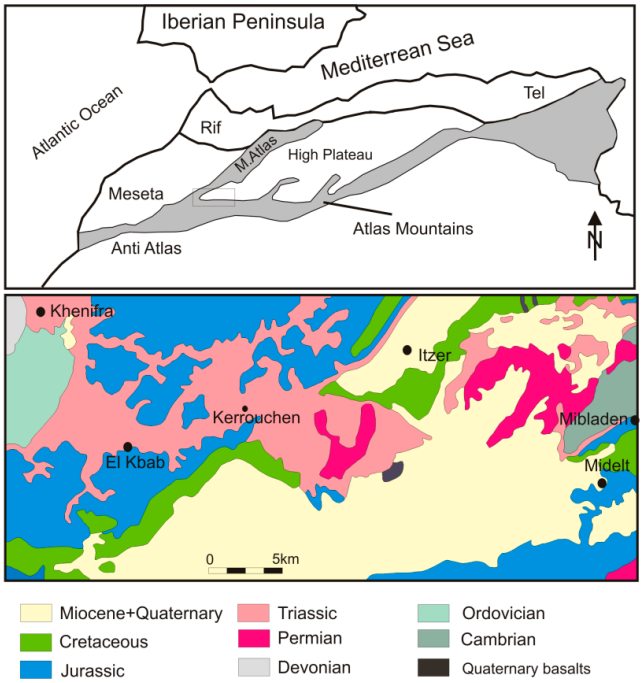

Figure 1. Simplified geological map of the Kerrouchen area, modified after Arboleya et al. [16]. Legend: Miocen and Quaternary: different sediments—alluvial sands, gravels and clays; Cretaceous: conglomerates, flysch, detritic facies; Jurassic: different limestones; Triassic: different types of limestones, basaltic volcanics with agates; Permian: acidic volcanics; Devonian: detritic facies; Ordovician: different shales; Cambrian: limestones and detritic facies.

3. Experimental Section

Agate samples representing all three morphological types were selected for the investigation. They were examined with binoculars in order to select the proper material for the research using the SEM-EDS, RS, and XRF methods.

3.1. Microscopic Analyses

Thin sections of all agate samples were examined with an Olympus BX 51 polarizing microscope (Olympus, Tokyo, Japan) with a magnification range from 40× to 400×. Backscattered electron (BSE) observations were performed on polished sections using an FEI Quanta 200 field emission gun scanning electron microscope equipped with energy-dispersive spectroscopy (FEI, Hillsboro, OR, USA). The system was operated at 20 kV accelerating voltage in low-vacuum mode. Scanning electron microscopy provided information on the distribution and quantity of solid inclusions found in agates and their general chemical composition. Combined with Raman spectroscopy, it enables identification of all mineral and organic phases found within an agate's matrix.

3.2. Raman Spectroscopy

Raman spectra of silica phases and the most pronounced solid inclusions were recorded using a Thermo Scientific DXR Raman microscope (Thermo Fisher, Waltham, MA, USA), equipped with 100-, 50- and 10× magnification objectives, operating in a confocal mode and working in the backscatter geometry. The polished sample pieces were excited with a 532 nm high-power laser. The laser focus diameter was 1–2 μm.

In the line-mapping experiments, 320 spectra with 50 μm steps were obtained for two monocentric and polycentric agates polished pieces. The most intensive bands for quartz (460 cm^{-1}) and moganite (501 cm^{-1}) in each point of the analytical grid were recorded.

3.3. X-Ray Fluorescence

Two-dimensional maps of elemental distribution were done with a laboratory micro-XRF setup. The setup utilizes a low-power X-ray tube with a Mo-target and silicon drift X-ray detector. Primary radiation from the X-ray tube is focused with a polycapillary lens—the nominal spot size is 16.4 μm full width at half maximum (FWHM). Detailed information about the setup can be found elsewhere [17]. The measurements were performed in standard 45°/45° geometry, where the angles between impinging beam, sample normal, and detector axis equalled 45°. The X-ray tube voltage and current were 50 kV and 1 mA, respectively. The sample surface was placed out of focus of the primary radiation beam, in order to achieve effective size of a beam of approximately 200 μm FWHM. The 300 μm slices of samples were mounted between two 2.5 μm thick Mylar films stretched across a plastic holder. The holder was placed on a motorized stage that allows sample positioning with micrometre resolution.

For the mapping of monocentric and polycentric agates the step size (pixel size), equal to 200 μm in the horizontal and vertical directions, was used. The first map consists of 104 × 141 pixels, equal to 20.8 × 28.2 mm^2. The second map was 139 × 136 pixels, or 27.8 × 27.2 mm^2. The sample acquisition times were 2.5 s per pixel and 3 s per pixel, respectively. The net intensities of the characteristic lines were calculated by nonlinear least-squares fitting with AXIL-QXAS software package. Correlations of Fe vs. Mn, Mn vs. Ti, Fe vs. Ti, and Cu vs. Mn were calculated only for analytical points measured inside the agate samples.

4. Results

The agates from Kerrouchen show a rich diversity of colours and morphological features. They range in size from 12 to 30 cm in diameter, and differ in internal structure, thickness of individual zones, colours, as well as patterns. Generally, they can be divided into three groups: monocentric, polycentric, and pseudostalactitic (Figure 2).

Generally, the monocentric agates are white-grey. They very rarely exhibit the infiltrative channel (*osculum*) (Figure 2A). Their external, very thin zones are likely composed of chalcedony, while the centre with thick layers could be built of fine individual quartz or chalcedony (Figure 2A,B). Locally, some monocentric agates contain additional red-brownish zones at the rim, which result from the scattered compounds of iron within a silica matrix (Figure 2G,H).

The polycentric (multi-eye) agates show a distinctive spotted appearance (Figure 2D). The spots contain red-pinkish concentric bands which are reminiscent of numerous “eyes” at the grey-brown silica background.

The pseudostalactite agates are characterized by a random, irregular arrangement of individual layers which resemble stalactite-like forms existing on the top or bottom of the rock (Figure 2C,I). They are generally coloured red, brown, and white. An aperture is located in the central part of most of these agates (Figure 2E,F,I).

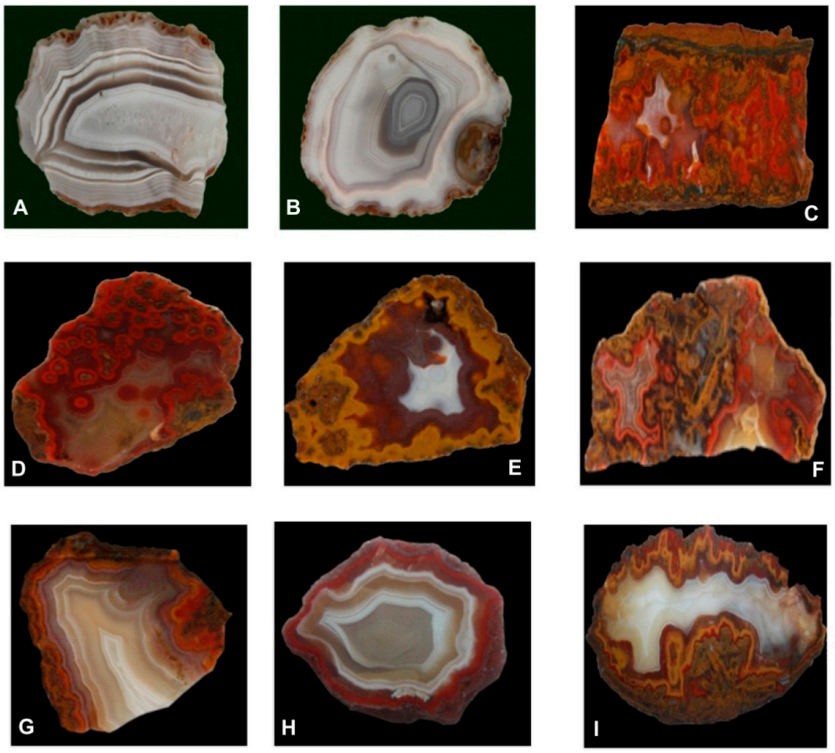

Figure 2. Kerrouchen agates: (**A**) monocentric agate with osculum, 3.5 × 5.5 × 2.9 cm, greyish white internal and reddish to dark-brown external zone; (**B**) monocentric agate, 3.2 × 4.1 × 2.1 cm, greyish white to pinkish internal and reddish to dark-brown external zone; (**C**) pseudostalactie agate, 3.2 × 5.8 × 1.1 cm, light-brown, reddish, orange to greyish-white interior and light-brown external zone; (**D**) polycentric agate, 6.1 × 4.5 × 1.5 cm, pink, red to orange interior and light-brown external zone; (**E**) pseudostalactite agate, 3.4 × 4.4 × 0.9 cm, orange, red, brown to greyish-white interior and light-brown external zone; (**F**) pseudostalactite agate, 2.9 × 6.6 × 1.3 cm, orange, red, brown to greyish-white interior and light-brown external zone; (**G**) monocentric agate, 3.5 × 6.0 × 1.3 cm, light-brown, orange to greyish-white interior and dark-brown external zone; (**H**) monocentric agate, 4.0 × 4.3 × 1.1 cm, light-brown to greyish-white interior and dark-brown to red external zone; (**I**) pseudostalactite agate, 6.2 × 11.5 × 0.5 cm, light-brown, orange to greyish-white interior and light-brown external zone.

4.1. Microscopic Observations

In monocentric and polycentric agates, the zones of different generations of silica are easily observed (Figure 3A,B,E,F). The external parts of agate nodules, at the contact with the host rock, are usually composed of fibrous and crypto-crystalline chalcedony, which locally form the sequence of minor laminas interleaving each other. The boundaries between the zones are sharp. In the inner parts of the nodules the youngest generation of silica (perfectly formed quartz) crystallized. Sometimes it is accompanied by opaque minerals and/or organic matter (Figure 3A,B,E,F). Locally, the infiltrative channel can be observed in the agates.

The presence of colouring compounds (iron oxides and/or hydroxides, carbonaceous matter) is variable in the agates. However, they mainly occur in polycentric and pseudostalactite varieties, whereas monocentric agates are significantly depleted of them. Generally, these pigments form randomly dispersed aggregates within fine-crystalline and spherulitic chalcedony (Figure 3C,D) or are concentrated along with the borders between the individual layers. In some agates' nodules, Fe-compounds cluster around spherulitic chalcedony grains (Figure 3E,F) forming characteristic concentric rings ("eyes"). In pseudostalactitic agates a mixture of Fe-compounds and organic matter concentrates in the stalactitic-like forms (Figure 3G,H).

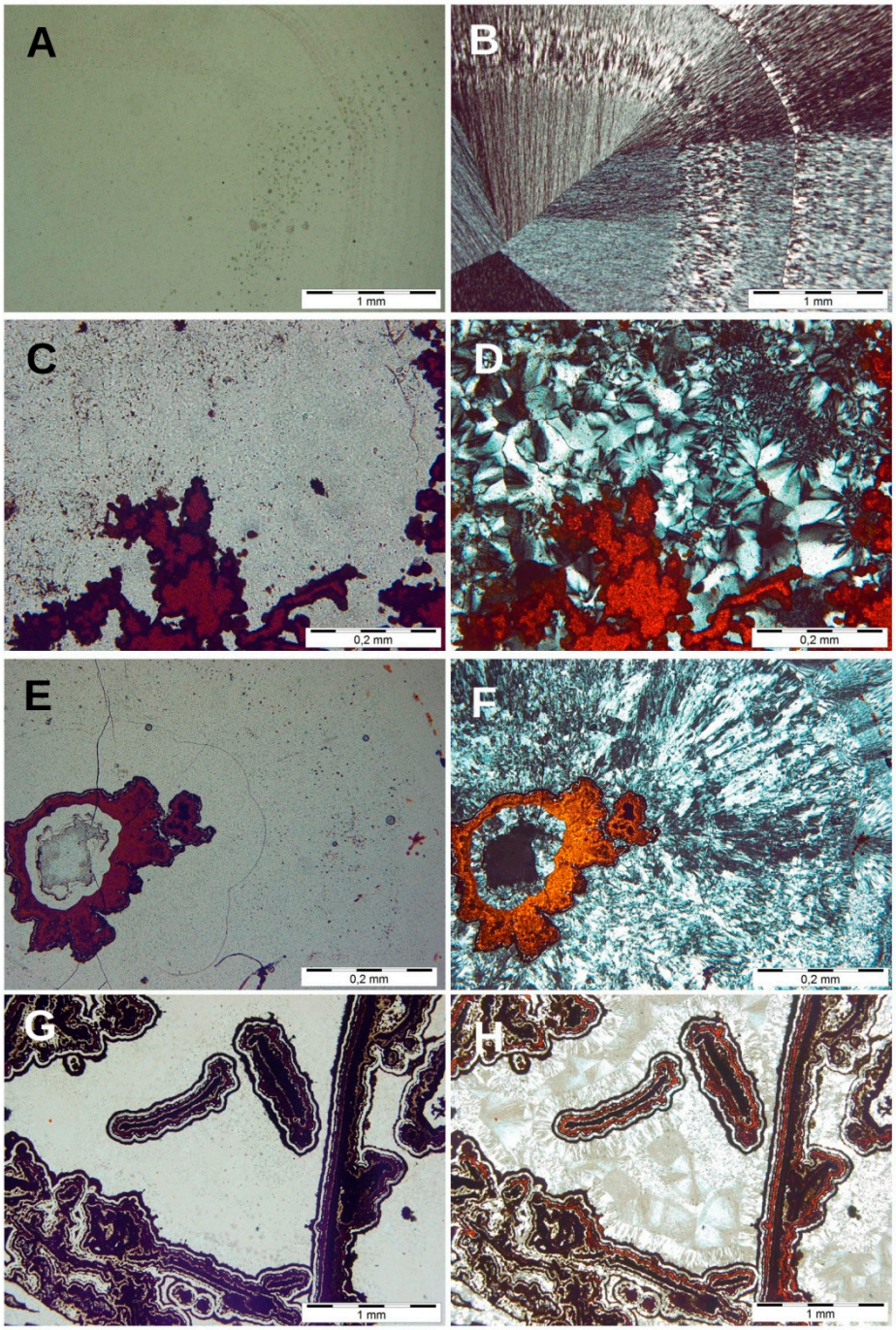

Figure 3. Images of microtextures in various agate types from Kerrouchen, observed in transmitted and polarized light; 1N and NX: monocentric (**A**,**B**); pseudostalactic (**C**,**D**,**G**,**H**); polycentric (**E**,**F**).

Agates' pigments can be observed under SEM. They form beautiful regular and irregular mosaics rich in ornamentation (Figure 4B,C). Their frequency of occurrence is variable and differs from sample to sample. The concentric rings are mainly built of a mixture of Fe compounds with silica (Figure 4A), whereas randomly dispersed pigments are composed of copper sulphides (light domain) and Fe-compounds (dark domain) (Figure 4D).

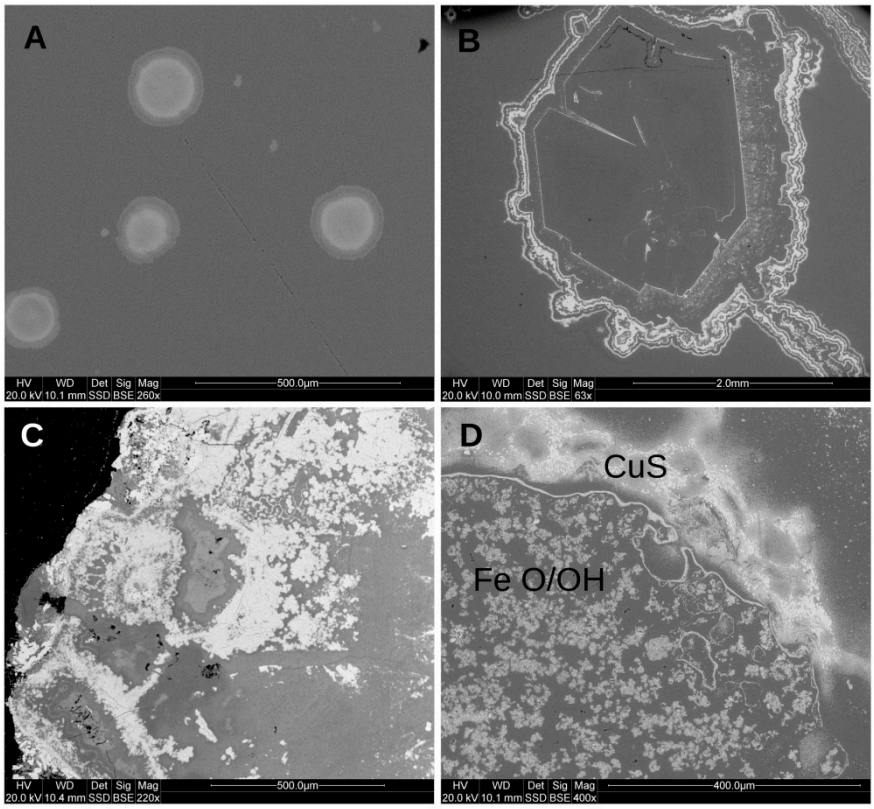

Figure 4. Backscattered electron (BSE) images of Fe compounds forming different aggregates (**A**,**B**,**C**) and locally accompanied by Cu sulphides (**D**) in agates from Kerrouchen.

4.2. Raman Microspectroscopy

Monocentric agates with white and grey bands consist mainly of low quartz and subordinately moganite with distinctive 460 and 501 cm^{-1} marker bands, respectively (Figure 5). Linear mapping of these agates indicated that moganite is distributed mainly in darker (grey) regions of the agates nodules, whereas low quartz is dominant in white regions of the nodules.

These agates are devoid of any solid inclusions. In contrast, polycentric agates with characteristic brown and red regions inside the nodule contain numerous Fe-compounds, mainly hematite and goethite. The presence of hematite is clearly marked by bands at 223, 245, 290, 408, 498, and 609 cm^{-1} (Table 1; Figure 6). The intensive bands at 290, 408, and 609 cm^{-1} are assigned to Fe-O symmetric bending vibrations (E_g mode), whereas the weaker bands at 223 and 498 cm^{-1} are related to symmetric stretching vibrations of Fe-O (A_{1g}) [18]. Hematite is accompanied by carbonaceous matter marked by D-band at 1320 and G-band at 1585 cm^{-1}, respectively (Table 1). The band at ca. 1320 seems to be a combination of two smaller bands: one attributed to carbonaceous matter which normally occurs at 1350 cm^{-1} [19] and the second one from hematite which normally appears at about 1300 cm^{-1} [20]. In this complex inclusion there are also traces of carbonates (possibly calcite). The 1085 cm^{-1} intensive peak was taken as a marker band.

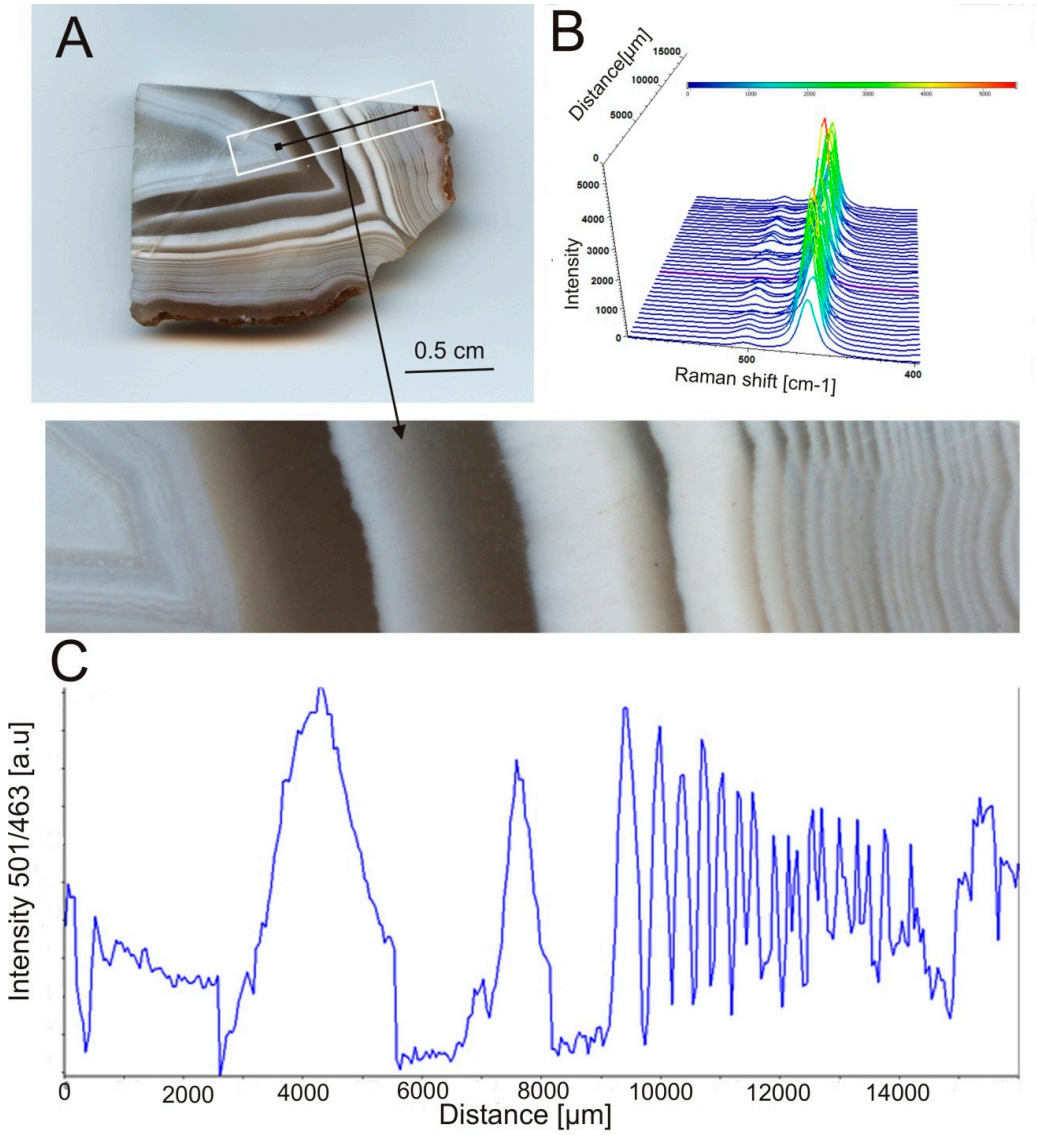

Figure 5. 3D (**B**) plots of micro-Raman line map of monocentric agate nodule from the center core towards the outer rim (**A**) with a diagram showing the ratio of the 501/463 intensities based on peak area measurements along the scan line (**C**).

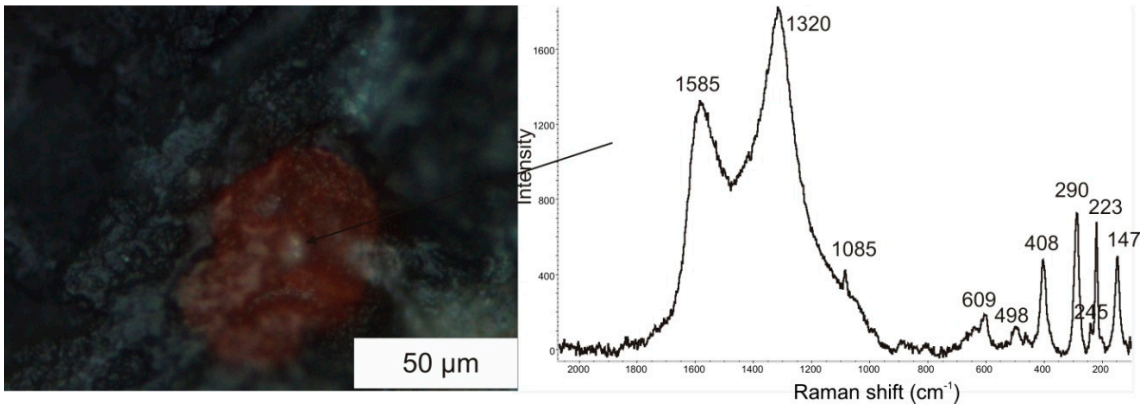

Figure 6. Microphoto of complex inclusion of hematite, calcite, and organic substance in agate with the related Raman bands.

Goethite found in agates is evidenced by marker bands at 297, 384, 415, 548, 680, 997, and 1298 cm^{-1} (Table 1; Figure 7). The most intensive band at 384 cm^{-1} is connected with Fe-O-Fe/-OH symmetric stretching vibrations. The others are attributed to Fe-OH symmetric bending and Fe-OH asymmetric stretching vibrations, respectively [18]. The bands at 203 and 463 cm^{-1} are attributed to low alpha quartz [21], which is the main mineral component of agates.

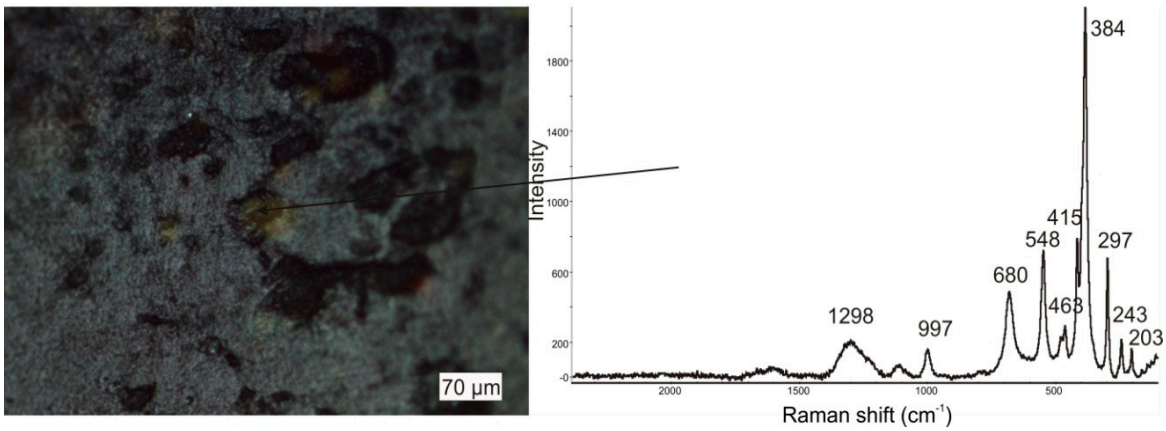

Figure 7. Microphoto of goethite in agate with its Raman spectrum.

Single crystals of rutile (Table 1; Figure 8) were also identified within the agates with characteristic bands at 141 (B_{1g}), 443 (E_g), and 610 cm^{-1} (A_{1g}). The distinctive broad band at 241 cm^{-1} in the rutile RS spectrum is a second order scattering effect [22].

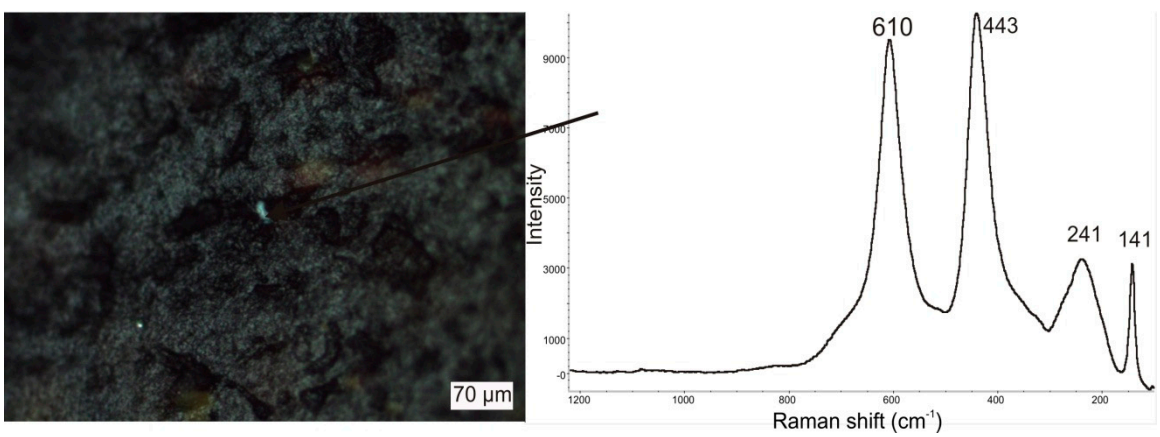

Figure 8. Microphoto of rutile in agate with its Raman spectrum.

Table 1. Raman bands (cm^{-1}) observed in spectra shown in Figures 6–8.

Band (cm^{-1})	Assignment	References
223, 245, 290, 408, 498, 609, 1320	hematite	[18]
1320, 1585	carbonaceous matter	[19]
1085	carbonates (possibly calcite)	[23]
297, 384, 415, 548, 680, 997, 1298	goethite	[18]
141, 443, 610	rutile	[22]

4.3. X-Ray Fluorescence

Two samples of monocentric and polycentric agate (Figure 2, samples H and D, respectively) were analysed with XRF to observe the distribution of elements such as Fe, Cu, Mn and Ti within

the agate matrix (Figures 9–11). For both samples, titanium and manganese concentrate very close to the outer rims of agate nodules, whereas iron is also distributed in the inner part of the nodules (Figures 9 and 11). Copper is deposited in a rhomboid structure that is the core of the polycentric agate and measures around 5 mm in size (Figure 9), whereas it is barely detected in the monocentric agate (Figure 11). Positive correlations were observed between manganese vs. iron and titanium in both agates (Figures 10 and 12). Interestingly, for monocentric agates, good correlation between Fe and Ti was also observed (Figure 12). There are no correlations between Cu and Mn, though their analytical points, forming rhombus shaped structures in the core of polycentric agate, are located near each other, but not in the same place (Figures 9 and 10).

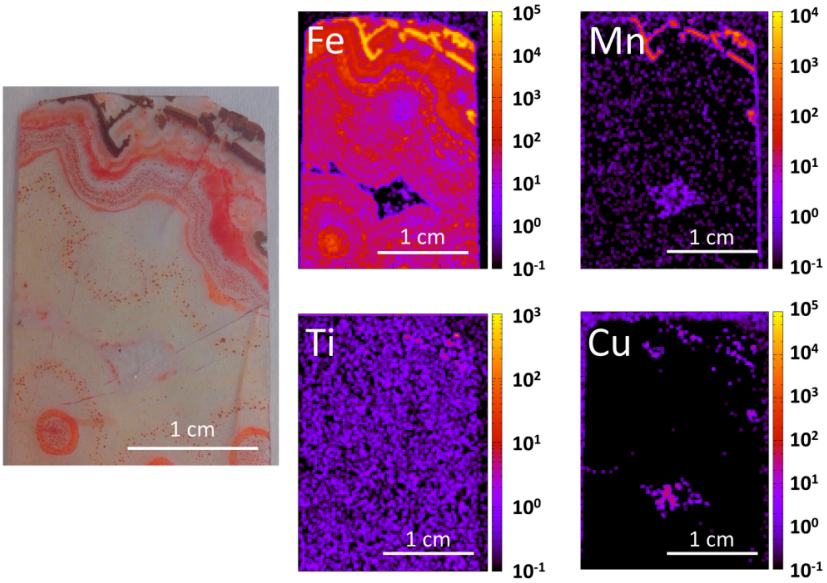

Figure 9. The photo of polycentric agate together with maps of characteristic Kα X-ray intensities showing spatial distribution of Fe, Mn, Ti and Cu.

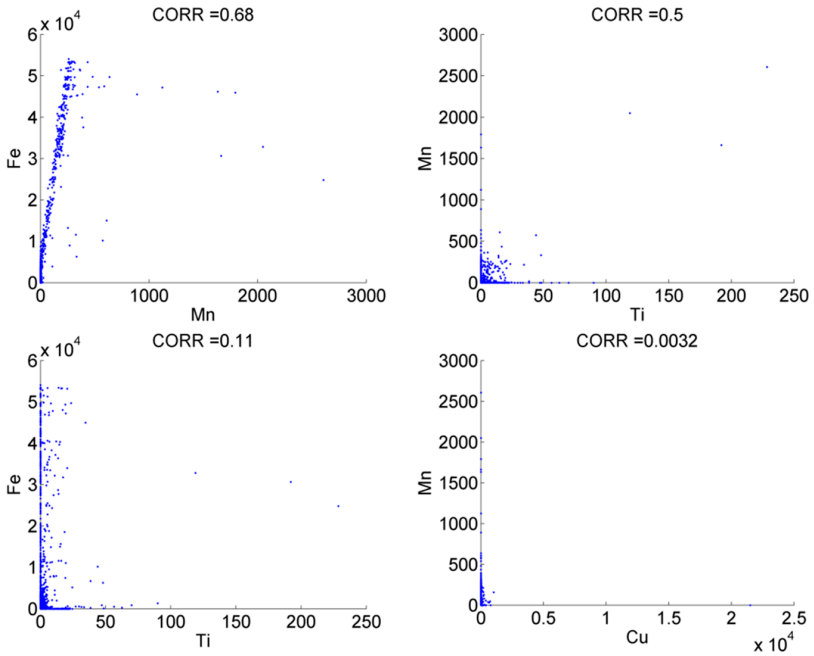

Figure 10. Correlations between characteristic X-ray intensities of Fe, Mn, Ti and Cu for polycentric agate.

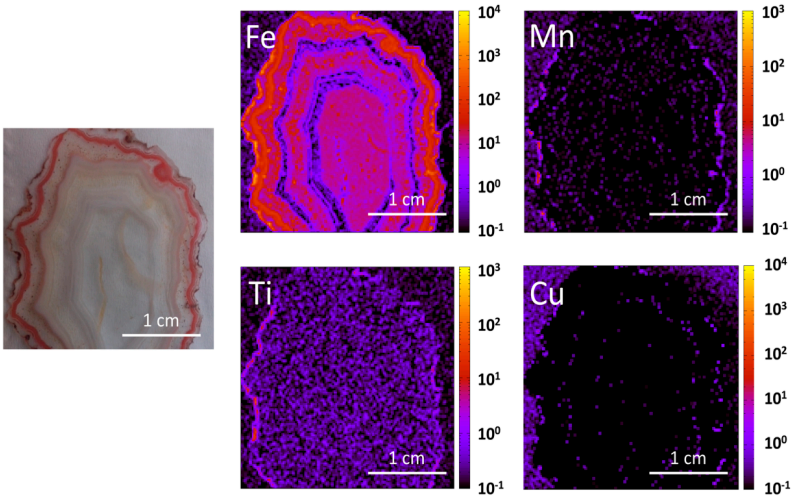

Figure 11. The photo of monocentric agate together with maps of characteristic Kα X-ray intensities showing spatial distribution of Fe, Mn, Ti and Cu.

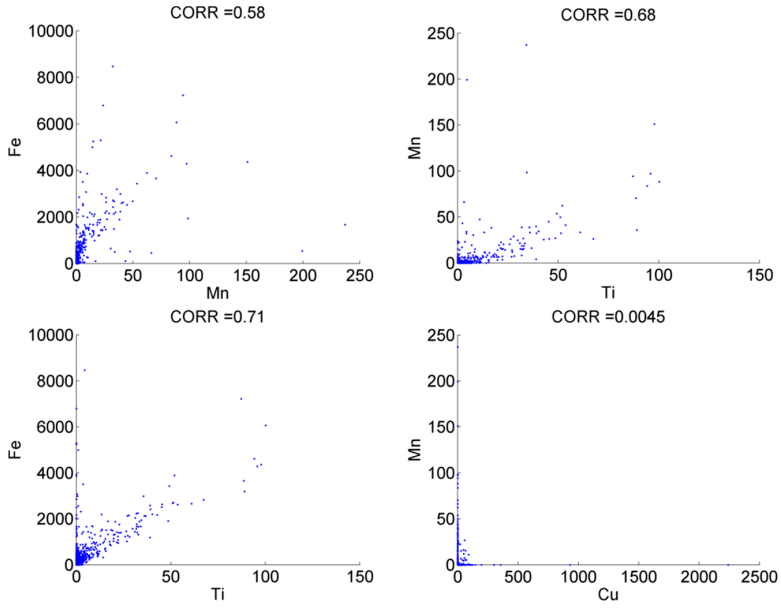

Figure 12. Correlations between characteristic X-ray intensities of Fe, Mn, Ti and Cu for monocentric agate.

5. Discussion

The agates from the Kerrouchen vicinity (Khénifra Province, Meknés-Tafilalet Region), occurring in Triassic basalts, display exceptionally high diversity in textural features and accessory compounds, forming solid inclusions. They exhibit richness in colour, morphology, and patterns. Among all agates varieties that have been found in that region so far, three different morphological groups of agates were distinguished: i.e., monocentric (samples A, B, G, and H), polycentric (sample D), and pseudostalactitic (samples C, E, F, and I). Rarely, they reveal specific morphological zones such as *osculum* or aperture. The agates are made up of almost two polymorphs of silica, i.e., mainly low quartz and subordinately moganite, which under polarizing microscope are described as chalcedony. The content of moganite within silica rocks increases from zero [1] to ~70% [24,25] along with their maturation (vide [3]). Moxon and Rios [26] noted that maturation of cryptocrystalline silica phases lowers the moganite content over tens of millions of years.

The silica in agates from Kerrouchen is accompanied by the presence of iron compounds such as hematite and goethite. They occur in a size range from tiny crystals to large aggregates. Fe-oxides and -hydroxides form regular, round, star-like aggregates or laminas sandwiched with pure silica. Locally, they are randomly distributed within the silica matrix. It seems that both Fe as well as Si probably originate from the same source, i.e., low temperature hydrothermal fluids and/or fluids from the alteration of host volcanics (e.g., [4,27]). The distribution of iron within the agates micro-texture might be both of primary or secondary origin. Iron oxides can admixture from amorphous silica during crystallization or can be removed from the silica and accumulated due to the ongoing growth in the growth zones of the gems. The positive correlations between iron vs. manganese, and titanium vs. manganese, are consistent with the geochemistry of these elements observed down to hydrothermal conditions.

Agates from Kerrouchen, though macroscopically different from agates from Sidi Rahal, contain a similar wealth of solid inclusions (hematite, goethite, rutile, and copper sulphides) formed during post-magmatic processes at the post magmatic activities (hydrothermal stage). They are the same age (Triassic) and occur in the same rock types (basalts) as agates from Sidi Rahal, so moganite contribution in them is similar (vide [3]). The only feature differentiating these stones is the presence of opal CT (cristobalite-tridymite), which was not identified in agates from Kerrouchen. In spite of some differences, these beautiful Moroccan gems from Sidi Rahal and Kerrouchen seem to have a common origin.

Summing up, the formation of agates from Kerrouchen was induced by Si-rich and Fe-moderate fluids. Sparse copper sulphides, titanium oxides as well as calcium carbonates were likely incorporated during post-magmatic processes. The origin of solid bitumen can be of hydrothermal or hypergenic processes by exposure to groundwater [3]. Regardless of its origin, organic matter seems to be a ubiquitous component of many gemstones, including agates [28–31].

Acknowledgments: Jacek Szczerba, Remigiusz Molenda, Andrzej Kuźma are gratefully acknowledged for providing the stones for the study. We also thank very much Jens Götze, two other anonymous Reviewers and Fan Wang, the Editor of Minerals, for their constructive criticism as well as friendly and helpful remarks, which significantly improved the manuscript. This work was supported by a research statutory grant No 11.11.140.319 from the AGH University of Science and Technology (Krakow, Poland).

Author Contributions: Lucyna Natkaniec-Nowak initiated the investigations of agates, designed the experiments and contributed to writing the paper. Magdalena Dumańska-Słowik analysed the data of micro-Raman analyses and contributed to writing the paper. Marek Lankosz and Paweł Wróbel performed XRF analyses and analyzed the data. Jaroslav Prsek provided with some materials and prepared the section 'geological setting'. Adam Gaweł performed microRaman and SEM analyses. Jacek Kocemba made microscopic photos and analyzed the data. Joanna Kowalczyk assisted in editing the text.

Conflicts of Interest: The authors declare no conflict of interest.

References

1. Moxon, T.; Nelson, D.R.; Zhang, M. Agate recrystallization: Evidence from samples found in Archaean and Proterozoic host rocks, Western Australia. *Aust. J. Earth Sci.* **2006**, *53*, 235–248. [CrossRef]
2. Heaney, P.J. A Proposed Mechanism for the Growth of Chalcedony. *Contrib. Mineral. Petrol.* **1993**, *115*, 66–74. [CrossRef]
3. Dumańska-Słowik, M.; Natkaniec-Nowak, L.; Wesełucha-Birczyńska, A.; Gaweł, A.; Lankosz, M.; Wróbel, P. Agates from Sidi-Rahal, in the Atlas Mountains, Morocco: Gemmological characteristics and proposed origin. *Gems Gemol.* **2013**, *49*, 148–159. [CrossRef]
4. Götze, J. Agate-fascination between legend and science. In *Agates III*; Zenz, J., Ed.; Bode Verlag GmbH: Salzhemmendorf, Germany, 2011; pp. 19–133.
5. Mayer, D. *Erlesene Achate. Exqusite Agates*; Bode Verlag: Haltern, Germany, 2013; pp. 1–424. (In German)
6. Jahn, S.; Bode, R.; Lycberg, P.; Medenbach, O.; Lierl, H.J. *Marokko—Land der Schönen Mineralien und Fossilien*; Bode Verlag: Haltern, Germany, 2003; pp. 1–536. (In German)
7. Zenz, J. *Achat-Schätze*, 1st ed.; Mineralien Welt: Salzhemmendorf, Germany, 2005; pp. 288–301. (In German)
8. Zenz, J. *Achate*; Bode Verlag: Haltern, Germany, 2005; pp. 1–656. (In German)

9. Zenz, J. *Achate II*; Bode Verlag: Haltern, Germany, 2009; pp. 1–656. (In German)
10. Gottschaller, S. Wichtige Mineralfundstellen in Marokko. In *Marokko*; ExtraLapis No. 42; Weise Verlag: Munich, Germany, 2012; pp. 76–98.
11. Mayer, D. "Nicht nur" Achate in Marokko. *ExtraLapis* **2012**, *42*, 22–25. (In German)
12. Mohr, C. Zur aktuellen Achat-Fundsituation in Marokko. *Miner. Welt* **2012**, *23*, 82–89. (In German)
13. Schwarz, D. Marokko-und dieses Mal keine Achate. *Miner. Welt* **2012**, *23*, 85–88. (In German)
14. Choubert, G.; Marais, J. Geologie du Marocco. In Proceedings of the 19th International Geological Congress, Algiers, Algeria, 8–15 September 1952 .
15. Laville, E. Role of the Atlas Mountains (northwest Africa) within the African-Eurasian plate-boundary zone: Comment. *Geology* **2002**, *30*, 1–95. [CrossRef]
16. Arboleya, M.L.; Teixell, A.; Charroud, M.; Julivert, M. A structural transect through the High and Middle Atlas of Morocco. *J. Afr. Earth Sci.* **2004**, *39*, 319–327. [CrossRef]
17. Wróbel, P.; Czyżycki, M.; Furman, L.; Kolasiński, K.; Lankosz, M.; Mrenca, A.; Samek, L.; Węgrzynek, D. LabVIEW control software for scanning micro-beam X-ray fluorescence spectrometer. *Talanta* **2012**, *93*, 186–192. [CrossRef] [PubMed]
18. Legodi, M.A.; De Wall, D. The preparation of magnetite, goethite, hematite and maghemite of pigment quality from mill scale iron waste. *Dyes Pigments* **2006**, *74*, 161–168. [CrossRef]
19. Jehlicka, J.; Beny, C. First and second order Raman spectra of natural highly carbonified organic compounds from metamorphic rocks. *J. Mol. Struct.* **1999**, *480*, 541–545. [CrossRef]
20. Laufente, B.; Downs, R.T.; Yang, H.; Stone, N. The power of databases: The RRUFF project. In *Highlights in Mineralogical Crystallography*; Armbruster, T., Danisi, R.M., De Gruyter, W., Eds.; W. De Gruyter: Berlin, Germany, 2015; pp. 1–30.
21. Götze, J.; Nasdala, L.; Kleeberg, R.; Wenzel, M. Occurrence and distribution of "moganite" in agate/chalcedony: A combined micro-Raman, Rietveld, and cathodoluminescence study. *Contrib. Mineral. Petrol.* **1998**, *133*, 96–105.
22. Swamy, V.; Muddle, B.C.; Dai, Q. Size-dependent modifications of the Raman spectrum of rutile TiO_2. *Appl. Phys. Lett.* **2006**, *89*, 1–3. [CrossRef]
23. Gunasekaran, S.; Anbalagan, G.; Pandi, S. Raman and infrared spectra of carbonates of calcite structure. *J. Raman Spectrosc.* **2006**, *37*, 892–899. [CrossRef]
24. Parthasarathy, G.; Kunwar, A.C.; Srinivasan, R. Occurrence of moganite-rich chalcedony in the Deccan flood basalts, Killari, Maharashtra, India. *Eur. J. Mineral.* **2001**, *13*, 127–134. [CrossRef]
25. Pop, D.; Constantina, C.; Tătar, D.; Kiefer, W. Raman spectroscopy on gem-quality microcrystalline and amorphous silica varieties from Romania. *Stud. UBB Geol.* **2004**, *49*, 41–52. [CrossRef]
26. Moxon, T.; Rios, S. Moganite and water content as a function of age in agate: An XRD and thermogravimetric study. *Eur. J. Mineral.* **2004**, *16*, 269–278. [CrossRef]
27. Moxon, T.; Reed, S.J.B. Agate and chalcedony from igneous and sedimentary hosts aged from 13 to 3480 Ma: A cathodoluminescence study. *Mineral. Mag.* **2006**, *70*, 485–498. [CrossRef]
28. Dumańska-Słowik, M.; Natkaniec-Nowak, L.; Kotarba, M.J.; Sikorska, M.; Rzymełka, J.A.; Łoboda, A.; Gaweł, A. Mineralogical and geochemical characterization of the "bitumineous" agates from Nowy Kościół (Lower Silesia, Poland). *Neues Jahrb. Miner. Abh.* **2008**, *184*, 255–268. [CrossRef]
29. Dumańska-Słowik, M.; Wesełucha-Birczyńska, A.; Natkaniec-Nowak, L. Inclusions in topaz from miarolitic pegmatites of the Volodarsk-Volynski Massif (Ukraine)—A Raman spectroscopic study. *Spectrochim. Acta A* **2013**, *109*, 97–104. [CrossRef] [PubMed]
30. Wesełucha-Birczyńska, A.; Natkaniec-Nowak, L. A Raman microspectroscopic study of organic inclusions in "watermelon" tourmaline from Paprok mine (Nuristan, Afghanistan). *Vib. Spectrosc.* **2011**, *57*, 248–253. [CrossRef]
31. Wesełucha-Birczyńska, A.; Słowakiewicz, M.; Natkaniec-Nowak, L.; Proniewicz, L.M. Raman microspectroscopy of organic inclusions in spodumens from Nilaw (Nuristan, Afghanistan). *Spectrochim. Acta A* **2011**, *79*, 789–796. [CrossRef] [PubMed]